Fisher equation for anisotropic diffusion: Simulating South American human dispersals

Luis A. Martino,[*,†] Ana Osella,[†] and Claudio Dorso[†]
Physics Department, FCEyN, Universidad de Buenos Aires, Argentina

José L. Lanata[‡]
Anthropology Department, FFyL, Universidad de Buenos Aires, Argentina
(Received 29 May 2007; published 27 September 2007)

The Fisher equation is commonly used to model population dynamics. This equation allows describing reaction-diffusion processes, considering both population growth and diffusion mechanism. Some results have been reported about modeling human dispersion, always assuming isotropic diffusion. Nevertheless, it is well-known that dispersion depends not only on the characteristics of the habitats where individuals are but also on the properties of the places where they intend to move, then isotropic approaches cannot adequately reproduce the evolution of the wave of advance of populations. Solutions to a Fisher equation are difficult to obtain for complex geometries, moreover, when anisotropy has to be considered and so few studies have been conducted in this direction. With this scope in mind, we present in this paper a solution for a Fisher equation, introducing anisotropy. We apply a finite difference method using the Crank-Nicholson approximation and analyze the results as a function of the characteristic parameters. Finally, this methodology is applied to model South American human dispersal.

DOI: 10.1103/PhysRevE.76.031923 PACS number(s): 87.23.Cc

I. INTRODUCTION

Reaction-diffusion models play an important role in the description of population dynamics. If we consider diffusion as a coherent movement interrupted by scattering events, then we can make the analogy with first migrations of human beings, which found during their dispersals different kinds of barriers which deviated and/or reoriented their movements. Migrations can be associated to a nonequilibrium state which can start from a localized external perturbation (for example, the irruption of a number of invaders at a localized point); then, this perturbation is spread via diffusion mechanisms to the neighboring regions, going from a stationary state to the propagation of a traveling wave. Thus this behavior can be described as a diffusive phenomenon plus a term which takes into account the rate of density population increase. Standard models applied Fisher's equation developed to describe the "wave of advance" of advantageous genes [1], generalized to the case of animal range expansion (e.g., Williamson [2]). The basic equation is given by [1]

$$\frac{dn}{dt} = f(n,K) + D\nabla^2 n, \tag{1}$$

where $n(r,t)$ corresponds to the local human population density (number of humans per unit area) at time t and position $r=(x,y)$. D stands for the diffusion parameter and K represents the environmental carrying capacity, which takes into account the potentiality of an environment to support human population on a sustained basis [3]. Both are functions of position. Finally, $f(n,K)$ describes the rate at which population increases and is usually represented, in ecology, by the logistic function [4]

$$f(n,K) = \alpha n\left(1 - \frac{n}{K}\right) \tag{2}$$

with α the intrinsic maximum population growth rate.

This equation has been widely studied, specially for unbounded systems (e.g., Abramson *et al.* [5]). Being a nonlinear equation, finding its solutions is in most cases a complex task. Several analytical methods have been developed to solve this equation. Some recent studies were discussed in Izús *et al.* [6]; King and McCabe [7]; Abramson *et al.* [5]; and Olmos and Shizgal [8]. The formal solution of one-dimensional (1D) models yields traveling wave states. When extended to two-dimensional (2D) and to three-dimensional (3D) models, the shape of the wave front may change during propagation and evolve to some stationary configuration. In 2D space, along with a plane wave, there exist other solutions, with different velocity of propagation. In particular, Brazhnik and Tyson [9] identified five different solutions for an unbounded, spatially uniform medium: plane wave, a space-oscillating propagation front, and three waves with different shapes and velocities. However, it is not usually possible to obtain exact analytical wave solutions, especially when boundary conditions are considered. Brazhnik and Tyson [10] solved the equation for the 2D system, considering an infinitely long stripe with no flux allowed through the boundaries. For this particular case they found that only two modes survive (plane and oscillating) because the front line of the wave must approach the boundary orthogonally. In another case, Izús *et al.* [6] solved the equation assuming a linear version of the equation, subjected to partially reflecting boundary conditions. Notwithstanding, for more complex geometries, the equation must be analyzed numerically. Different approaches have been used, for example, by means of

*lmartino@df.uba.ar
†Also at CONICET, Argentina.
‡Also at CEBBAD, CONICET, and F.F. de Azara.

integral methods (Feng and Li [11]), finite elements (Gunzburger *et al.* [12]), and finite differences (Pao [13]).

In particular, this equation was used to model Paleoindian dispersal in North America (Steele *et al.* [14]). These authors solved Eq. (1) for a 2D system using finite differences, assuming that the three parameters, D, α, and K could be estimated from "ethnographic and archaeological information." D and α were maintained constant while K was varied according to the environmental properties.

In this work we applied this formalism to model the human dispersal in South America. Specifically, we wanted to model time and mode of human dispersion into the new environments. Recently, Lanata and García [15] proposed that the diffusion coefficient of the different paleoenvironments for human dispersion, together with the use of environmental corridors, could have differentiated two metapopulations, Andean and Amazonian. On the other hand, in the desert and semidesert temperate lowlands of the South American Southern Cone and Patagonian region both populations could coexist in a mixed situation. This kind of evolution could not be described using the formalism as it was applied by Steele *et al.* [14].

The reason for such a failure can be traced to the fact that one of the main constraints of this model is the assumption of a constant diffusion coefficient. This assumption produces a dispersion that evolves as a radial wave front, analogous to the dispersion in a isotropic medium. On the contrary, the actual situation is that the diffusion should depend on the characteristics of not only the habitat where the individuals are but also of the neighboring places toward which they intend to move.

This condition has not been considered previously for modeling hominid dispersion. In fact, few analyses have been done regarding an anisotropic behavior in Fisher's equation (e.g., Elmer and Van Vleck [16]; Krishnan *et al.* [17]; and Lanata *et al.* [18]). Then, we solved the reaction-diffusion Fisher's equation introducing anisotropy. We analyzed the wave-front development for different characteristics of the system and compared the results to those obtained using the isotropic equation. Finally, we modeled the dispersion of paleoindian in South America, constraining the model with archeological and paleoenvironmental data.

In Sec. II we describe the solution of the equation under anisotropic conditions and we tested the approximation in a simple model. In Sec. III we describe the anthropologic data. In Sec. IV we show the simulations for the South American region. Finally in Sec. V conclusions are drawn.

II. ISOTROPIC VERSUS ANISOTROPIC DIFFUSION MODEL

The finite-difference method using the Crank-Nicholson approximation was applied in order to solve the differential equation; this method uses a double step in the time domain for the calculation of spatial derivatives. The spatial derivatives at time $t+\Delta t$ were obtained using Euler's approach for time t and time $t+\Delta t/2$. In the time domain the method uses a simple forward difference.

The system is divided into rectangular cells (i,j) in which a is the length of the cell in the x direction and b is the length of the cell in the y direction; then for each cell, Eq. (1) can be written as

$$\frac{dn_{i,j,t+\Delta t} - dn_{i,j,t}}{\Delta t} = A(n_{i,j,t}) + B(n_{i,j,t,\Delta t/2}). \tag{3}$$

The first term $A(n_{i,j,t})$ is associated to the population growth.

$$A(n_{i,j}) = \alpha n_{i,j}\left(1 - \frac{n_{i,j}}{K_{i,j}}\right). \tag{4}$$

The second one $B(n_{i,j,t,\Delta t/2})$ is associated with diffusion, and in the isotropic case D is constant and then the resulting equation is

$$\begin{aligned} B(n_{i,j,t,\Delta t/2}) = {} & \frac{D}{a^2}(n_{i+1,j,t} - 2n_{i,j,t} + n_{i-1,j,t}) \\ & + \frac{D}{b^2}(n_{i,j+1,t} - 2n_{i,j,t} + n_{i,j-1,t}) \\ & + \frac{D}{a^2}(n_{i+1,j,t+\Delta t/2} - 2n_{i,j,t+\Delta t/2} + n_{i-1,j,t+\Delta t/2}) \\ & + \frac{D}{b^2}(n_{i,j+1,t+\Delta t/2} - 2n_{i,j,t+\Delta t/2} + n_{i,j-1,t+\Delta t/2}) \end{aligned} \tag{5}$$

with

$$n_{i+1,j,t+\Delta t/2} = n_{i,j,t} + \frac{D\Delta t}{2b^2}(n_{i+1,j+1,t} - 2n_{i+1,j,t} + n_{i+1,j-1,t}). \tag{6}$$

In a similar way, we can calculate the terms $n_{i-1,j,t+\Delta t/2}$, $n_{i,j,t+\Delta t/2}$, $n_{i,j+1,t+\Delta t/2}$, and $n_{i,j-1,t+\Delta t/2}$ and then Eq. (5) can be rewritten as

$$\begin{aligned} \Delta t B(n_{i,j,t}) = {} & s_x(1-4s_y)(n_{i+1,j,t} - 2n_{i,j,t} + n_{i-1,j,t}) + s_y(1-4s_x) \\ & \times (n_{i,j+1,t} - 2n_{i,j,t} + n_{i,j-1,t}) + s_y s_x(n_{i+1,j+1,t} \\ & + n_{i+1,j-1,t} + n_{i-1,j+1,t} + n_{i-1,j-1,t} - 4n_{i,j,t}), \end{aligned} \tag{7}$$

where s_x and s_y are given by

$$s_x = \frac{D\Delta t}{a^2},$$

$$s_y = \frac{D\Delta t}{b^2}. \tag{8}$$

If the cell is taken square, we have that $a=b=h$, $s_x=s_y=s$, and Eq. (7) adopts the form

$$\begin{aligned} \Delta t B(n_{i,j,t}) = {} & s(1-2s)(n_{i+1,j,t} + n_{i-1,j,t} + n_{i,j+1,t} + n_{i,j-1,t} \\ & - 4n_{i,j,t}) + s^2(n_{i+1,j+1,t} + n_{i+1,j-1,t} + n_{i-1,j+1,t} \\ & + n_{i-1,j-1,t} - 4n_{i,j,t}). \end{aligned} \tag{9}$$

It can be shown that for $s=1/6$, the approximation is of fourth order [19], then Eq. (9) becomes

$$\Delta t B(n_{i,j,t}) = \frac{D}{h^2}\sum_{l=1}^{8} w_l(n_l - n_{i,j}), \tag{10}$$

where, for a cell (i,j), $n_{i,j}$ is the population in the cell, $n_{i,j,l}$ is the population for one of the l nearest neighbors (eight neighbors, including the diagonal cells); h^2 is the area of the cell (i,j), and w_l is a weight factor that defines if the neighboring cell l shares a side or a vertex. The migrations to the diagonal neighbors are associated with a double migration process, for example, a migration to the upwards-left vertex may be given by a first migration leftward and a second migration upwards.

We can define a normalized diffusion coefficient $d=\frac{D}{h^2}$; then the diffusion term in Eq. (3) results:

$$B(n_{i,j}) = d\sum_{l=1}^{8} w_l(n_l - n_{i,j}). \tag{11}$$

The migration was normalized in such a way that all the inhabitants of a cell migrate to the closest neighbors if they are empty, in which case $d\Delta t=1$ for a stationary population ($\alpha=0$).

To introduce an anisotropic behavior, we used the most general form of Fisher's equation [Eq. (1)]:

$$\frac{dn}{dt} = f(n,K) + \nabla D \nabla n. \tag{12}$$

If we apply finite differences dividing the space into square cells (i,j), the anisotropy can be introduced if we think that every lattice has associated an individual diffusion parameter and carrying capacity. For a nine neighbor scheme centered in cell (i,j) the arrangement is shown in Fig. 1.

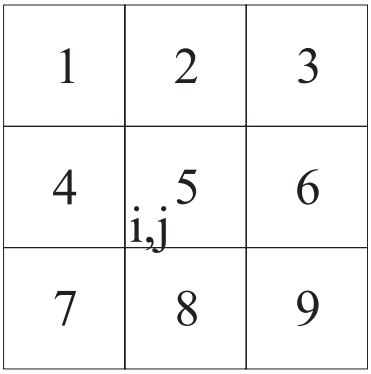

FIG. 1. Nine neighbor scheme for a lattice centered in a (i,j) cell.

Following the suggestion introduced in [14], we define a diffusion coefficient for each pair of cells through the following relation: $\bar{D}_{l,k}=\sqrt{D_l D_k}$ in which D_l carries information about the local properties of cell l. This definition is consistent with the case in which, if a given cell l is completely inaccessible, $D_l=0$ and then all diffusion coefficients $\bar{D}_{l,k}$ pointing toward that cell are zero.

Using the nine point technique in a square mesh, the diffusion term for the cell (i,j) of Eq. (12) results:

$$\begin{aligned}
&\frac{\Delta t}{2h^4}[(\bar{D}_{1,2}\bar{D}_{2,5} + \bar{D}_{1,4}\bar{D}_{4,5})(n_1 - n_5) + (\bar{D}_{3,2}\bar{D}_{2,5} + \bar{D}_{3,6}\bar{D}_{6,5})(n_3 - n_5) + (\bar{D}_{7,4}\bar{D}_{4,5} + \bar{D}_{7,8}\bar{D}_{8,5})(n_7 - n_5) \\
&+ (\bar{D}_{9,6}\bar{D}_{6,5} + \bar{D}_{9,8}\bar{D}_{8,5})(n_9 - n_5)] + \bar{D}_{2,5}\left[\frac{1}{h^2} - \frac{\Delta t}{2h^4}(\bar{D}_{1,2} + \bar{D}_{3,2} + \bar{D}_{4,5} + \bar{D}_{6,5})\right](n_2 - n_5) \\
&+ \bar{D}_{4,5}\left[\frac{1}{h^2} - \frac{\Delta t}{2h^4}(\bar{D}_{1,4} + \bar{D}_{7,4} + \bar{D}_{2,5} + \bar{D}_{8,5})\right](n_4 - n_5) + \bar{D}_{6,5}\left[\frac{1}{h^2} - \frac{\Delta t}{2h^4}(\bar{D}_{3,6} + \bar{D}_{9,6} + \bar{D}_{2,5} + \bar{D}_{8,5})\right](n_6 - n_5) \\
&+ \bar{D}_{8,5}\left[\frac{1}{h^2} - \frac{\Delta t}{2h^4}(\bar{D}_{7,8} + \bar{D}_{9,8} + \bar{D}_{4,5} + \bar{D}_{6,5})\right](n_8 - n_5).
\end{aligned} \tag{13}$$

If we analyze each term separately we can clearly seen that migrations to the diagonal neighbors are associated with a double migration; for example, migration from cell 5 to cell 1 depends on the term $\bar{D}_{1,2}\bar{D}_{2,5}+\bar{D}_{1,4}\bar{D}_{4,5}$, which indicates that there exist two ways to reach cell 1: a first one passing through cell 2 and a second one passing through cell 4.

To see the effect of anisotropy in a simple case, we solved the equations for a three-layer model. We assumed a rectangular space formed by three parallel bands, each one with different values of the diffusion constant D. Keeping in mind that our goal was the modeling of human dispersion, we assigned to the parameters of the model values related to this application. The external borders of the cell are such that no flux occurs across them. On the other hand, migration across the inner borders is allowed. The reaction focus is an initial population located at a center point close to the left border. We assumed $\alpha=0.03$, which means a 3% annual growth rate and a constant carrying capacity $K=20$.

We first performed the calculations for the isotropic formulation [Eqs. (3)–(11)]. In this case, a value of $d=0.5$ was assigned to $d_{i,j}$. In Fig. 2 we show the development of migration with time. We can see that the wave front evolves as

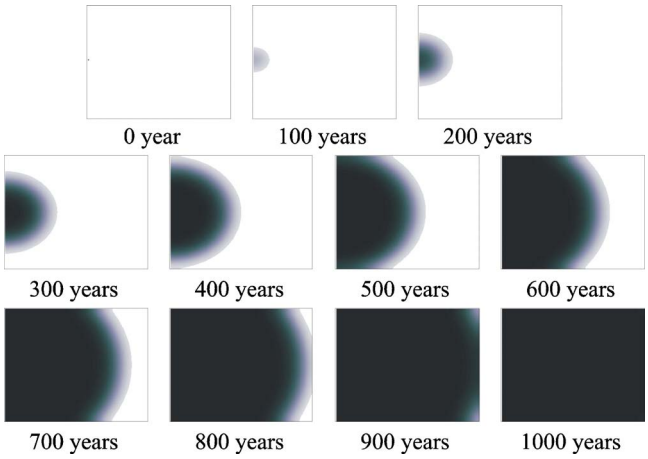

FIG. 2. (Color online) Calculations for isotropic media.

a radial wave up to the time in which one of the outer borders is reached. From there on, it monotonically advances until the whole region is filled.

We then used the anisotropy formulation [Eq. (13)] for a model characterized by the sequence $D_1=400$, $D_2=200$, and $D_3=300$ from top to bottom (these values are related to typical paleopopulation densities for America [14]). See Fig. 3.

The results of such a calculation are displayed in Fig. 4. Comparing the resulting evolution patterns with those obtained for isotropic diffusion, we can see that the main difference appears in the velocity in advance of the front wave; migration is delayed in regions of lower D values, producing a distortion in the shape of the wave front modifying the way in which each rectangular space is populated.

The next step is the inclusion of corridors. We design them as narrow layers parallel to each interface, along which migration is favored. To better visualize these effects we show in Fig. 5 the difference in the advance of the wave front, with and without corridors.

For the example shown here, differences became noticeable from approximately 400 years, when the effect of lager velocities along the corridors produce a clear difference in the migration pattern close to the interfaces. These results indicate that, with an adequate set of parameters, different models for dispersal of population can be built up.

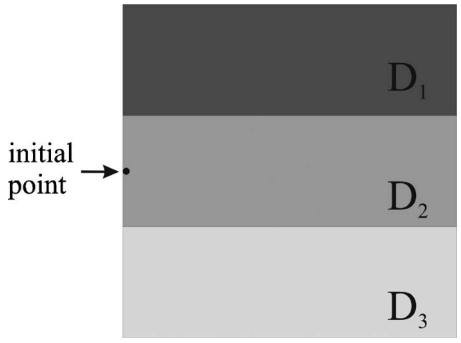

FIG. 3. Arrangment used for anisotropic calculations.

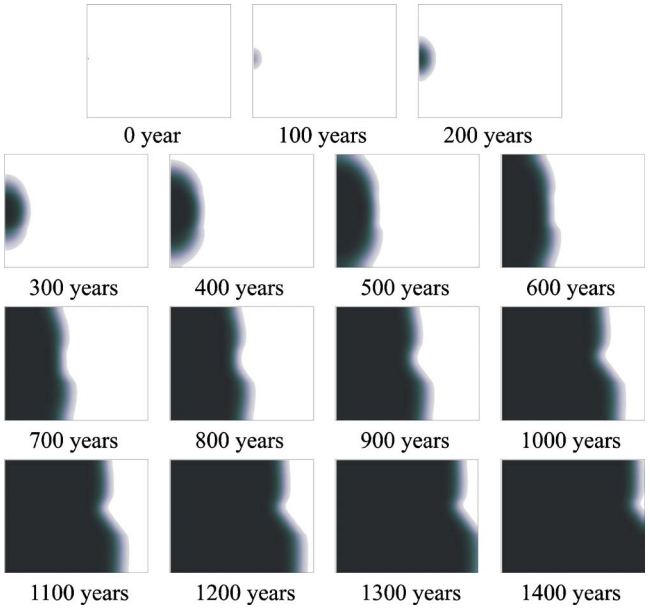

FIG. 4. (Color online) Calculations for anisotropic media. $D_1=400$, $D_2=200$, and $D_3=300$.

III. DATA AND MODELING PARAMETERS

The evidence of human dispersal in North and Central America indicates that hunter-gatherer populations entered through Beringia, the terrestrial bridge which joined Asia and America at different periods during the Late Pleistocene, previously to 18 000 rcybp (radiocarbon years before present). This is based on the evidence provided by the Broken Mammoth site, located in Alaska, and by other sites of the region. On the other hand, the dispersion in South America, according to present data, could only take place through Darien in

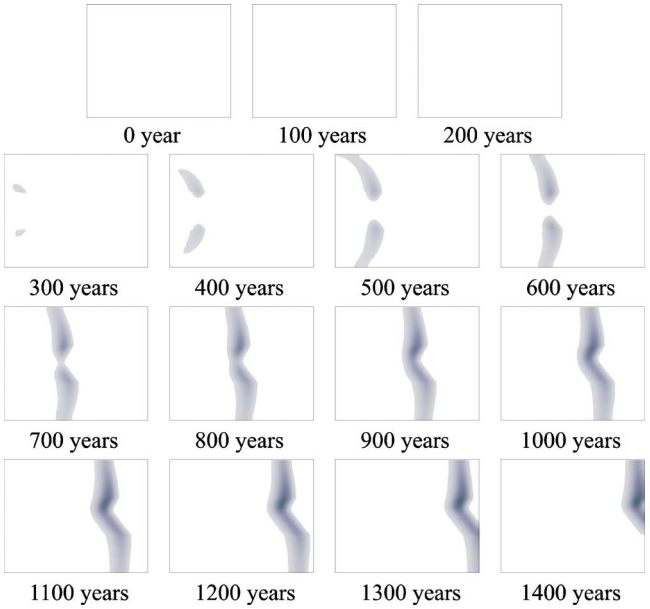

FIG. 5. (Color online) Obtained pattern for the difference in the wave front between simulations with and without corridors.

TABLE I. Early archeological sites in South America.

Archaeological site	Actual location	Date in rcybp
El Jobo	Venezuela	14 000
Taima Taima and Muaco	Venezuela	14 000
Pedra Furada and Sitio do Meio	Brazil	14 000
Monte Verde	Chile	13 700
Piedra Museo	Argentina	12 700
Cerro La China	Argentina	12 300
Lagoa Santa and Lapa Vemelha	Brazil	12 000
Lapa do Boquete	Brazil	12 000
Santana do Riacho	Brazil	11 900
Cueva del Medio	Chile	11 500
Fell's Cave	Chile	11 000
Turrialba	Costa Rica	11 000
Madden Lake	Panama	11 000
Quebrada Jagauy	Peru	11 000
Pedra Pintada	Brazil	11 000
Quebrada Tacahuay	Peru	10 700
Tres Arroyos	Chile	10 600
El Inga	Ecuador	9000
Toca da Esperanca	Brazil	6500

Panama. From the population dynamics perspective, Costa Rica and Panama acted like bottlenecks in such a way that the entrance of humans in South America constituted a kind of starting point for dispersal in a new continent (see [20] for an extensive revision of paleoindian sites).

The available South American archeological information came from excavations performed across the continent. Though controversies appear regarding the time when human dispersal began, it is generally aged between 18 000 and 14 000 rcybp (there are a few sites with radiocarbon dating previous to 18 000 rcybp, but they are still not reliable) [20,21]. In Table I the archeological data available at present is shown; the sites, with their correspondent actual location and the oldest dating found in each of them, are included.

It is interesting to remark that it is also possible that the dispersion could have been much quicker if we consider, for example, some early datings obtained at Monte Verde, located in the Patagonian Pacific coast [20]. This increase in the rate of advance could be explained with the assumption of the Pacific Ocean environmental corridor [15], in addition with a better use of marine resources [22]; but due to the rise of sea level during the Holocene, all archeological evidence should remain buried under the Pacific Ocean and then no archeological evidence could be obtained to support that assumption. Nevertheless, it is a hypothesis that is worthwhile to consider when performing the simulations.

The human dispersal depended on the characteristics of the environment, then adequate reconstructions are needed to perform the numerical modeling. We used the paleoenvironmental maps obtained by Adams [23]. This author reconstructed the paleovegetation distribution for different periods between the Last-Pleistocene and Early-Holocene (Fig. 6).

Those paleoenvironmental maps recognize 18 different habitats. To assign the corresponding carrying capacities, we

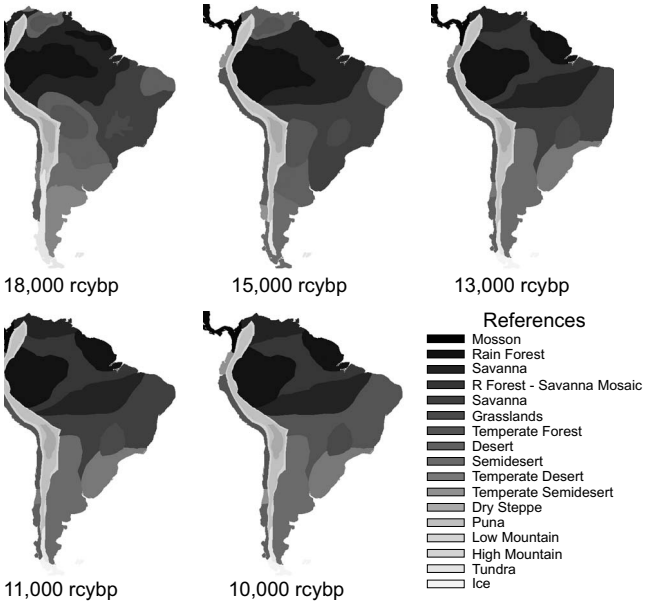

FIG. 6. Paleovegetation maps of South America at 18 000, 14 000, 12 000, 11 000, and 10 000 rcybp.

performed an analogy with similar actual characteristics, considering also that the density population varies from one habitat to another, in a way similar to the corresponding recent South American native populations [24,25]. Using this procedure, we assigned a density of 1.8 inhabitants per 100 km^2 in the Patagonian desert, 19.9 in the Venezuela fields, and 51.3 in the Matto Grosso forest. The complete ranking for the 18 habitats is displayed in Table II.

Following the principles of Patch theorem [26] a population stays in a habitat while they have sustained resources

TABLE II. Values for coefficients K and D for each habitat.

Environment	Carrying capacity K	Normalized diffusion constant D
Rain forest	16	700
Mosson	15	550
RFSM[a]	17	600
Savanna	18	800
Semidesert	2	100
Desert	1	50
Scrub	12	450
Grasslands	14	800
Dry steppe	11	250
Temperate forest	13	500
Temperate semidesert	3	150
Temperate desert	4	100
Low mountain	8	300
High mountain	5	400
Puna	7	200
Tundra	6	350
Ice	0	0

[a]RFSM: Rain Forest Savanna Mosaic.

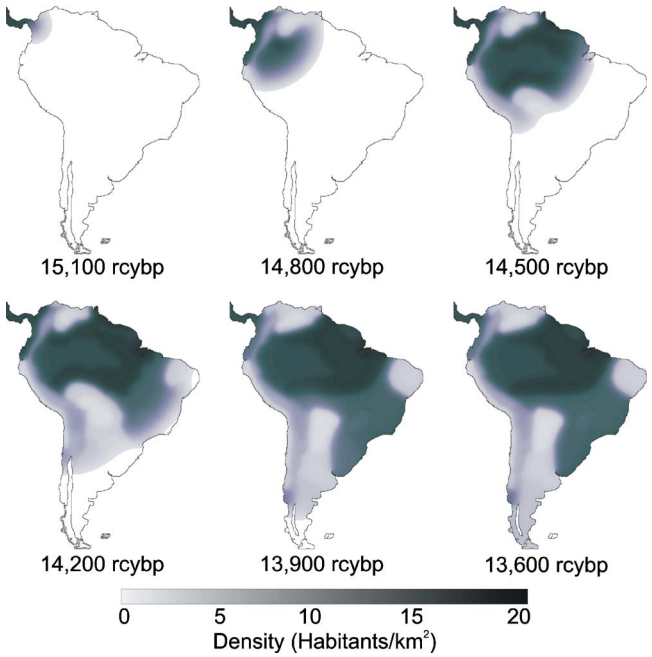

FIG. 7. (Color online) Human dispersal maps using the isotropic model.

and begin to migrate when these resources diminish. During the initial steps of dispersal, or occupation of new habitats, inhabitants can migrate before arriving at the limit density population. Moreover, frontiers between different habitats, named environmental corridors, present special advantages for a species in an invasion and/or dispersal stage. One of the main advantage of these corridors is that people there have access to more diversified resources, as different foods and basic elements can be obtained from the two or more habitats that form the corridor. Thus when a resource diminishes in one habitat, they can have quick access to equivalent or alternative resources from another habitat; and this characteristic may favor dispersion. This is particularly important in South America. Here three corridors may be clearly defined, a coastal one, along the Pacific Ocean, and two along both sides of the Andean Range also in the North-South direction. On the other hand, in the Amazonian region the corridors are widely separated and located along the West-East direction. If these corridors play effectively a role in hunter-gatherer dispersion, then the Pacific corridor should produce a faster dispersion than the movements through the Amazon. Also, preliminary craniometrical data seems to show a population affinity along the Andes on one side and the Amazon on the other [27].

IV. NUMERICAL SIMULATION RESULTS

The parameters necessary to perform the numerical simulations are α, which is related to the stationary increase of population, the diffusion coefficient D, and the environmental carrying capacity K, which is included in both processes. Also we need a starting date for beginning the dispersion, together with the corresponding habitat distribution for each time.

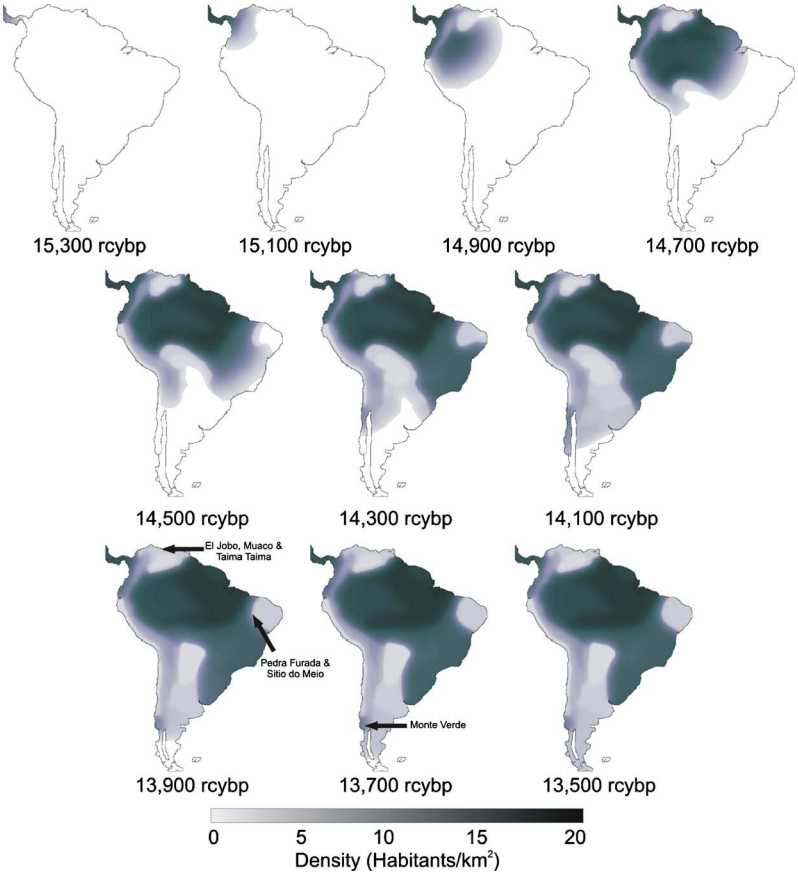

FIG. 8. (Color online) Human dispersal maps using anisotropic diffusion, with $\alpha=0.03$. Blacks arrows indicate an archeological date satisfied.

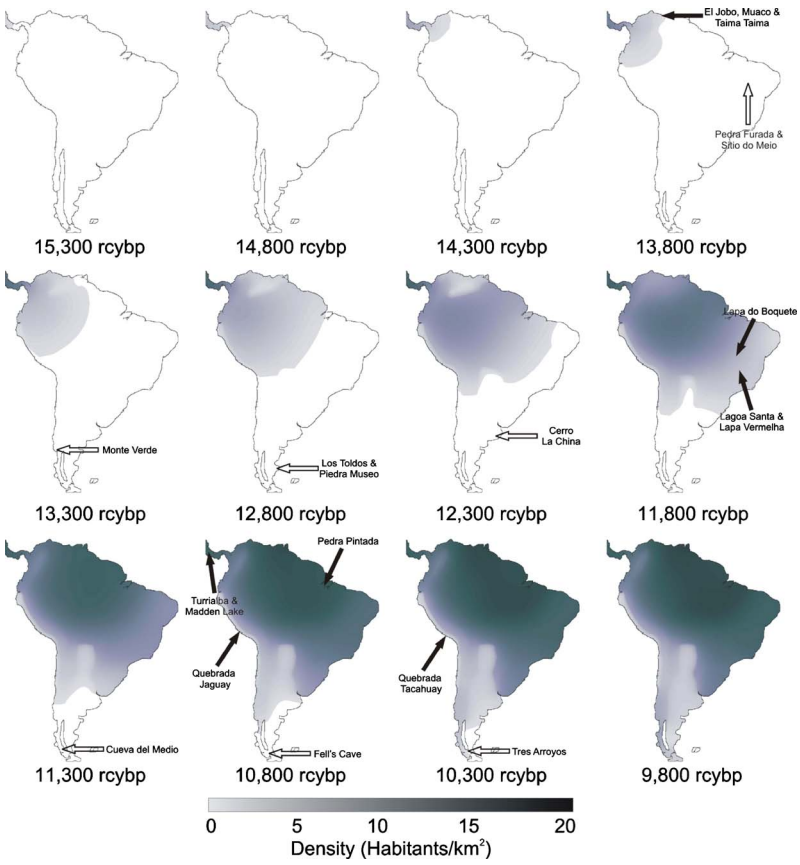

FIG. 9. (Color online) Human dispersal maps using anisotropic diffusion, with $\alpha=0.003$. Blacks arrows indicate an archeological date satisfied and white arrows indicate an archeological date not satisfied.

In the previous section we have described the usual values for most of these parameters; the discussion about the diffusion coefficient is remaining. In fact, this is basically the term that we have modified in the evolution equation.

The coefficient D_l represents the mobility in a particular habitat. [28] proposed that D_l is proportional to the square of the distance traveled in an environment between birth and death, (λ_i), and inverse to the time required to cover it (τ):

$$D_l = \frac{\lambda_i^2}{4\tau}. \tag{14}$$

This dependency was obtained if we assumed a 2D random walk. For our simulations the maximum mobility implies that the evolution was done with a $t=1$ month step.

To define the values for the carrying capacity, we used the paleoenvironmental maps, shown in Fig. 6. These maps were digitalized in cells equivalent to pixels. Then each cell has an area of 125.5 km^2.

A. Standard model

Steele [14] assumed $d_{i,j}=1$ and $\alpha=0.03$, for modeling paleoindian dispersion in North America. Then, at a first stage, we also assumed also an isotropic dispersion with $\gamma_{i,j,l}=1$, using these values for d and α. The values for K were selected from Table II.

To obtain the initial time for our simulations, we performed first an evolution through North America, assuming that dispersal started in Beringia, when America was joined to Asia during a glacial period. We obtained that the origin for South America dispersion should be at 15 kybp (see also [14]).

Figure 7 shows the results of evolution, assuming the parameters previously described. It can be observed that South America is covered in 1800 years. Also, all the archeological dates are satisfied. We modified the value of α; the main effect appears when it diminishes, producing a corresponding decrease in the velocity of advance. The main feature of the numerical simulation is that the dispersion evolves as a radial wave front, as expected, and then no crossover between populations is obtained; but this result is in contradiction with observed data that suggest the coexistence of different groups.

B. Anisotropic diffusion

We solve the anisotropic system for South America assigning values to coefficient $\bar{D}_{l,k}$ and the carrying capacity K according to the characteristics of the different environments. The complete list is shown in Table II.

We also included existence of corridors that were naturally distributed in the environment interfaces. In these corridors, the diffusion coefficient takes a value of $D=800$.

We accounted for different scenarios to the dispersal of South America. First, we simulated a dispersion with a large population growth rate $(\alpha=0.03)$; afterwards we used a small population growth rate $(\alpha=0.003)$, and finally we considered a second dispersal focus.

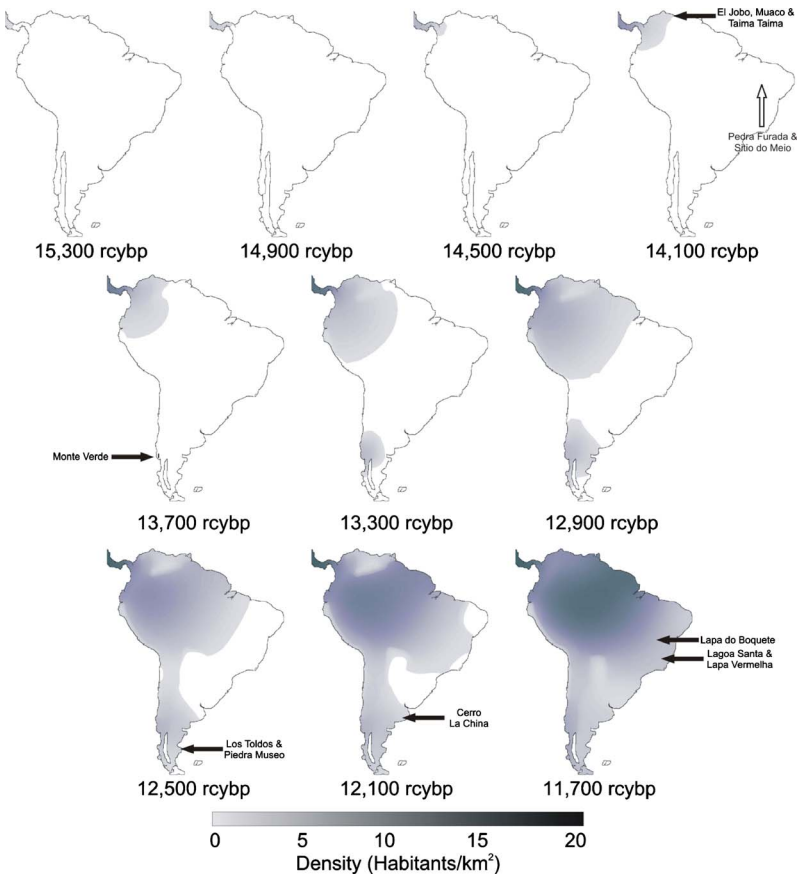

FIG. 10. (Color online) South American human dispersal maps using anisotropic diffusion, with $\alpha=0.003$, including a dispersal focus at Southern Chile. Blacks arrows indicate an archeological date satisfied and white arrows indicate an archeological date not satisfied.

1. $\alpha=0.03$

Figure 8 displays the results for this evolution process. As before, the region is covered in 1800 years. Also, as before, all the archeological dates are satisfied (only the sites in corresponding dates appear in the maps).

It is interesting to see that the wave front is no more uniform, but divides into two waves; this effect was given by the anisotropic diffusion and the environmental corridors. One of the wave fronts advances following the Pacific corridor while the other travels along the Matto Grosso forest, crossing over at the Chaco region, and from there evolves as a unique wave front. This fact was a remarkable coincidence with craniometrical data discussed in Sec. III.

2. $\alpha=0.003$

We show in Fig. 9 the evolution maps for $\alpha=0.003$. It can be seen that 7000 years are required to completely cover the continent, the velocity being four times smaller than the value obtained for $\alpha=0.03$.

It can be seen that archeological dates from Patagonia locations and the earlier data of Brazil are not satisfied. Moreover, it can also be seen that, as evolution is so slow, the wave front advances without producing crossovers and no metapopulation appeared. This facts indicates that a small population growth rate is not compatible with the archeological data.

3. Introduction of a secondary dispersal focus

Another scenario with a low population growth rate is one that considers that the old dates in South Chile could be due to a displacement through the Pacific coastal corridor, avoiding to enter in the more desert zones of the continent. Thus we simulated this. We maintained the hypothesis that the paleoindians entered through the actual Panama 15 000 rcybp, but we superposed another point of dispersion at South Chile, between 13 900 and 13 700 rcybp (assuming that the time difference was necessary for advancing through the coastal corridor). The evidence of the Monte Verde site [20] (see also Table I) should be the result of a fast coastal hunter-gatherer invasion and/or dispersals—maybe with canoes [22]—through the Pacific environmental corridors, but evidence could be under water.

In Fig. 10 we show the dispersion maps, obtained using $\alpha=0.003$; we used this value for α because a larger value should imply that Monte Verde's zone should have been occupied at 13 700 rcybp, and consequently a second focus of dispersion could not be distinguished.

The results show that two wave fronts crossover at the Central region of South America and the archeological dates are satisfied. There are, however, others aspects of this simulation which remain in conflict. If we assume that South America is a very good environment for hominid dispersal, then values of growth rates should be higher than the one required to fulfill both the archeological dates and the crossover of migration streams.

V. SUMMARY AND CONCLUSIONS

Isotropic diffusion usually applied for modeling human dispersion, which results in a radial wave front, cannot ex-

plain the way in which South America was occupied. Specially, evidence of crossover in population cannot be reproduced with this model.

To overcome this limitation, we solved the diffusion term of the dispersion equation including the dependence of the diffusive parameter, D, with the characteristics of the habitats. By applying the Crank-Nicholson scheme and assuming that $\bar{D}_{l,k}$ can be written as $\sqrt{D_l D_k}$, we obtained Fisher's equation, which explicitly take into account the different path needs to reach diagonal cells. This dependency produces an anisotropy; clearly, when migration from cell (i,j) takes place, the direction to the cell l with better conditions will be preferred.

We also took into account the introduction of corridors, along which mobility is higher than within each habitat. The result of this assumption is also an anisotropy, since dispersion along those corridors is preferred over transversal directions to less favorable environments.

Simulating a three-layer model, we analyzed the evolution of the wave front for different characteristics of each layer. We observed that, for isotropic diffusion, the wave front is not distorted and evolves in a monotonically increasing way. When we introduced anisotropy, the wave fronts were distorted and for some special cases delay appeared, producing a deformation in the advancing wave. Finally, when corridors are introduced, the wave front present delays due to the fact that advancing along them is privileged with respect to other paths.

This effect was remarkable when modeling the human dispersion in South America. When we applied the isotropic model, the wave front evolved radially, but when we introduced anisotropy, it resulted in a distortion that corresponded to a crossover of populations which is in accordance with some archeological evidence.

To further analyze the dependency of the dispersion velocity on the α parameter, we assumed two different values, with an order of magnitude of differences, and we observed a faster occupation for the largest value. Moreover, for this particular case, α values smaller than 0.003 produced a delay in the arriving times that contradicts chronological evidence.

We also included a second external perturbation to analyze how the resulting pattern is modified. We based our simulation on the fact that it is possible to consider that the old dates in South Chile could be due to a displacement through the Pacific coastal corridor, avoiding entering in the more desert zones of the continent. Thus we simulated this possibility, maintaining the hypothesis that the humans entered through the actual Panama 15 rcybp, but we superposed another point of dispersion at South Chile from where they could migrate, mixing with the streams coming through inland. With an adequate value for α, the crossover between populations could be also obtained. Nevertheless, this crossover is obtained only for a low growth rate, which could be in contradiction with the favorable environment that presented the continent.

In particular, regarding the contribution to archeology and anthropology, these numerical simulations constitute a starting point to study the mechanisms that ruled the dynamics of human dispersal in South America.

Based on the presented simulations we can assume that human dispersal in South America could have the following major features.

It was a relatively quick one, between 1500 and 2000 years long.

Environmental corridors could have played an important role by speeding up the process.

The initial average population rate growth for the whole continent could not be very low since it would not allow one to grasp the archeological data for the Late Pleistocene at the South Cone.

The pattern of anisotropic fast dispersion seems to best support the presence of at least two metapopopulations—Andean and Amazon—which appears to agree with the available paleoanthropological skull data.

It is clear that this kind of model implies the management of many parameters whose values should be estimated and/or modified to satisfy the available evidence; but it has the further benefit of allowing the analysis of the consequences that arise when multiple variables interact in different ways [29].

ACKNOWLEDGMENTS

This work was supported by the ANPCyT (Agencia Nacional de Promoción Científicca y Tecnológica) and CONICET (Consejo Nacional de Investigaciones Cientificas y Técnicas).

[1] R. A. Fisher, Ann. Eugen. **7**, 355 (1937).
[2] M. Williamson, *Biological Invasions* (Chapman and Hall, London, 1996).
[3] R. E. Dewar, Am. Anthropol. **86**, 1565 (1984).
[4] J. D. Murray, *Theoretical Biology* (Springer-Verlag, Berlin, 1990).
[5] G. Abramson, A. R. Byshop, and V. M. Kenkre, Phys. Rev. E **64**, 066615 (2001).
[6] G. Izús, R. Deza, C. Borzi, and H. S. Wio, Physica A **237**, 135 (1997).
[7] J. R. King and P. M. McCabe, Proc. R. Soc. London, Ser. A **459**, 2529 (2002).
[8] D. Olmos and B. D. Shizgal, J. Comput. Appl. Math. **193**, 219 (2006).
[9] P. K. Brazhnik and J. J. Tyson, SIAM J. Appl. Math. **60**, 371 (2000).
[10] P. K. Brazhnik and J. Tyson, J. Phys. A **32**, 8033 (1999).
[11] Z. Feng and Y. Li, Physica A **366**, 115 (2006).
[12] M. D. Gunzburger, L. S. Hou, and W. Zhu, J. Math. Anal. Appl. **313**, 419 (2006).
[13] C. V. Pao, J. Comput. Appl. Math. **136**, 227 (2001).
[14] J. Steele, J. Adams, and T. Sluckin, World Archaeol. **300**(2),

286 (1998).
[15] J. L. Lanata and A. García, in Paper presented at the 70th Annual Meeting of the Society for American Archaeology in Salt Lake City, UT, 2005 (unpublished).
[16] C. E. Elmer and E. S. Van Vleck, Appl. Numer. Math. **20**, 157 (1996).
[17] J. Krishnan, K. Engelborghs, M. Bär, K. Lust, D. Rose, and I. G. Kevrekidis, Physica D **154**, 85 (2001).
[18] J. L. Lanata, A. García-Herbst, L. Martino, and A. Osella, in *The Peopling of South-America*, edited by R. Kipnes and P. De Blassis (University Sao Paulo, Brazil, 2006).
[19] Medhi Dehghan, Nonlinear Anal. **48**, 637 (2002).
[20] T. Dillehay, *Monte Verde: A Late Pleistocene Settlement in Chile: The Archaeological Context and Interpretation* (Smithsonian Institute Press, Washington, DC, 1997).
[21] S. J. Fiedel, J. Archaeol. Res. **8**, 39 (2000).
[22] E. J. Dixon, *Bones, Boats, and Bison: Archeology and the First Colonization of Western North America* (University of New Mexico Press, Albuquerque, 2000).
[23] J. Adams, *South America during the Last 150.000 Years,* http://www.esd.ornl.gov/projects/qen/nercSOUTH AMERICA.html, 1998.
[24] L. R. Binford, *Constructing Frames of Reference: An Analytical Method for Archaeological Theory Buildings Ethnographic and Environmental Data* (University of California Press, Berkeley, 2001).
[25] R. L. Kelly, *The Foraging Spectrum* (Smithsonian Institution Press, Washington, DC, 1995).
[26] D. W. Stephens and J. R. Krebs, *Foraging Theory* (Princeton University Press, Princeton, 1987).
[27] H. Pucciarelli (private communication).
[28] A. J. Ammerman and L. L. Cavalli-Sforza, *The Neolithic Transition and Genetics of Populations in Europe* (Princeton University Press, Princeton, 1984).
[29] F. García, M. Moraga, S. Vera, H. Henríquez, E. Llop, E. Aspillaga, and F. Rothhammer, Am. J. Phys. Anthropol. **129**, 473 (2006).